

AFRL-PR-WP-TP-2006-252

**A MICROWAVE-AUGMENTED
PLASMA TORCH MODULE
(POSTPRINT)**

**S.P. Kuo, Daniel Bivolaru, Skip Williams, and
Campbell D. Carter**



MARCH 2006

Approved for public release; distribution is unlimited.

STINFO COPY

© 2006 IOP Publishing Ltd.

The U.S. Government is joint author of the work and has the right to use, modify, reproduce, release, perform, display, or disclose the work.

**PROPULSION DIRECTORATE
AIR FORCE MATERIEL COMMAND
AIR FORCE RESEARCH LABORATORY
WRIGHT-PATTERSON AIR FORCE BASE, OH 45433-7251**

REPORT DOCUMENTATION PAGE				<i>Form Approved</i> OMB No. 0704-0188	
<p>The public reporting burden for this collection of information is estimated to average 1 hour per response, including the time for reviewing instructions, searching existing data sources, gathering and maintaining the data needed, and completing and reviewing the collection of information. Send comments regarding this burden estimate or any other aspect of this collection of information, including suggestions for reducing this burden, to Department of Defense, Washington Headquarters Services, Directorate for Information Operations and Reports (0704-0188), 1215 Jefferson Davis Highway, Suite 1204, Arlington, VA 22202-4302. Respondents should be aware that notwithstanding any other provision of law, no person shall be subject to any penalty for failing to comply with a collection of information if it does not display a currently valid OMB control number. PLEASE DO NOT RETURN YOUR FORM TO THE ABOVE ADDRESS.</p>					
1. REPORT DATE (DD-MM-YY) March 2006		2. REPORT TYPE Journal Article Postprint		3. DATES COVERED (From - To) 09/21/2004 – 07/12/2005	
4. TITLE AND SUBTITLE A MICROWAVE-AUGMENTED PLASMA TORCH MODULE (POSTPRINT)				5a. CONTRACT NUMBER In-house	
				5b. GRANT NUMBER	
				5c. PROGRAM ELEMENT NUMBER 61102F	
6. AUTHOR(S) S.P. Kuo (Polytechnic University) Daniel Bivolaru (NASA Langley Research Center) Skip Williams and Campbell D. Carter (AFRL/PRAS)				5d. PROJECT NUMBER 2308	
				5e. TASK NUMBER AI	
				5f. WORK UNIT NUMBER 01	
7. PERFORMING ORGANIZATION NAME(S) AND ADDRESS(ES) Polytechnic University Department of Electrical & Computer Engineering Six Metrotech Center Brooklyn, NY 11201 ----- NASA Langley Research Center Hampton, VA 23681-2199				8. PERFORMING ORGANIZATION REPORT NUMBER AFRL-PR-WP-TP-2006-252	
Propulsion Sciences Branch (AFRL/PRAS) Aerospace Propulsion Division Propulsion Directorate Air Force Research Laboratory Air Force Materiel Command Wright-Patterson Air Force Base, OH 45433-7251					
9. SPONSORING/MONITORING AGENCY NAME(S) AND ADDRESS(ES) Propulsion Directorate Air Force Research Laboratory Air Force Materiel Command Wright-Patterson AFB, OH 45433-7251				10. SPONSORING/MONITORING AGENCY ACRONYM(S) AFRL-PR-WP	
				11. SPONSORING/MONITORING AGENCY REPORT NUMBER(S) AFRL-PR-WP-TP-2006-252	
12. DISTRIBUTION/AVAILABILITY STATEMENT Approved for public release; distribution is unlimited.					
13. SUPPLEMENTARY NOTES © 2006 IOP Publishing Ltd. The U.S. Government is joint author of the work and has the right to use, modify, reproduce, release, perform, display, or disclose the work. Journal article published in Plasma Sources Science and Technology, Vol. 15 (2006), pg. 266-275, Institute of Physics Publishing publisher. PAO case number: AFRL/WS 05-1243; Date cleared: 23 May 2005.					
14. ABSTRACT A new plasma torch device which combines arc and microwave discharges to enhance the size and enthalpy of the plasma torch is described. A cylindrical-shaped plasma torch module is integrated into a tapered rectangular cavity to form a microwave adaptor at one end, which couples the microwave power injected into the cavity from the other end to the arc plasma generated by the torch module. A theoretical study of the microwave coupling from the cavity to the plasma torch, as the load, is presented. The numerical results indicate that the microwave power coupling efficiency exceeds 80%. Operational tests of the device indicate that the microwave power is coupled to the plasma torch and that the arc discharge power is increased. The addition of microwave energy enhances the height, volume and enthalpy of the plasma torch when the torch operates at a low airflow rate, and even when the flow speed is supersonic, a noticeable microwave effect on the plasma torch is observed. In addition, the present design allows the torch to be operated as both a fuel injector and igniter. Ignition of ethylene fuel injected through the centre of a tungsten carbide tube.					
15. SUBJECT TERMS Supersonic combustion, plasma enhanced combustion, plasma torch, plasma igniter					
16. SECURITY CLASSIFICATION OF:			17. LIMITATION OF ABSTRACT: SAR	18. NUMBER OF PAGES 16	19a. NAME OF RESPONSIBLE PERSON (Monitor) Dr. Skip Williams 19b. TELEPHONE NUMBER (Include Area Code) N/A
a. REPORT Unclassified	b. ABSTRACT Unclassified	c. THIS PAGE Unclassified			

A microwave-augmented plasma torch module

S P Kuo¹, Daniel Bivolaru², Skip Williams³ and Campbell D Carter³

¹ Department of Electrical & Computer Engineering, Polytechnic University, Six Metrotech Center, Brooklyn, NY 11201, USA

² NASA Langley Research Center, Hampton, VA 23681-2199, USA

³ Air Force Research Laboratory, Propulsion Directorate, Wright-Patterson AFB, OH 45433, USA

Received 12 July 2005, in final form 11 January 2006

Published 22 March 2006

Online at stacks.iop.org/PSST/15/266

Abstract

A new plasma torch device which combines arc and microwave discharges to enhance the size and enthalpy of the plasma torch is described.

A cylindrical-shaped plasma torch module is integrated into a tapered rectangular cavity to form a microwave adaptor at one end, which couples the microwave power injected into the cavity from the other end to the arc plasma generated by the torch module. A theoretical study of the microwave coupling from the cavity to the plasma torch, as the load, is presented. The numerical results indicate that the microwave power coupling efficiency exceeds 80%. Operational tests of the device indicate that the microwave power is coupled to the plasma torch and that the arc discharge power is increased. The addition of microwave energy enhances the height, volume and enthalpy of the plasma torch when the torch operates at a low airflow rate, and even when the flow speed is supersonic, a noticeable microwave effect on the plasma torch is observed. In addition, the present design allows the torch to be operated as both a fuel injector and igniter. Ignition of ethylene fuel injected through the centre of a tungsten carbide tube acting as the central electrode is demonstrated.

(Some figures in this article are in colour only in the electronic version)

1. Introduction

Plasma sources having open structures are critical for applications requiring plasmas to be exposed to ambient conditions. The applications include spray coating and materials synthesis [1–3], decontamination of chemical and biological warfare agents [4–6] and ignition in hydrocarbon-fuelled combustors [7–9]. The application most relevant to the device described in this paper is ignition and combustion enhancement in hydrocarbon-fuelled supersonic combustors. For a typical hydrocarbon-fuelled supersonic combustor startup scenario [10, 11], the fuel–air mixtures will not auto ignite and some ignition aide is necessary to initiate main-duct combustion. The residence time through a typical combustion region is short, ~ 1 ms, and aids to reduce the ignition delay time and increase the rate of combustion of hydrocarbon fuels are essential to the operation of the combustor. To fulfil the

purpose, an ignition aid has to provide adequate energy to initiate the fuel/air mixture, and the delivered energy should be able to deeply penetrate into the supersonic crossflow.

A dense plasma jet can be produced through dc or low frequency capacitive [12, 13] or high frequency inductive arc discharges [14] which require adding flowing gas to stabilize the discharges. The gas flow also carries generated plasma out of the discharge region to form an extended plasma plume, thereby creating a torch module. The inductive torch and non-transferred dc torch employ high current power supplies and require external cooling to achieve stable operation. Consequently, the structures of these torches are relatively large and are therefore unsuitable for certain applications. The torch module patented by Kuo *et al* [15] can run in dc or low frequency ac mode and can produce low power (hundreds of watts) [16] or high power (a few kilowatts in 60 Hz periodic mode or hundreds of kilowatts in pulsed mode) [17] plasma

torches. The size of the plasma torch produced by this module depends on the gas flow rate. An increase in the gas flow rate increases the size as well as the cycle energy (in the case of periodic operation) of the plasma torch. However, the large flow rates decrease the average gas temperature, which may not be beneficial for some applications. Therefore, there is a need to develop new plasma sources which operate at atmospheric pressure conditions with less dependence on the gas flow rate.

Microwave power can be used to produce an electrodeless discharge resulting in a relatively large volume plasma with no need to flow gas through the discharge. However, in order to apply a microwave plasma in a designated region away from the source, special attention must be paid to ionization along the propagation path before reaching the preferred ionization region. The undesirable ionization causes attenuation and reflection of the microwave power possibly resulting in transmitted powers too low to cause air breakdown in the desired region [18]. Usually, a high Q resonant cavity is used to localize microwave discharge that produces microwave plasma inside the cavity [19]. A tapered rectangular waveguide [20] has also been used to spatially localize the microwave discharge. A gas flow is used to blow the microwave plasma out of an exit hole on the cavity/waveguide wall to form a plasma torch. Using high Q cavity, the required Q -factor limits the size of the hole, which in turn limits the diameter of the torch. On the other hand, if seed plasma is introduced, the microwave power density along the propagation path can be maintained below the breakdown threshold to assist the existing discharge, rather than to initiate a discharge, without the associated losses. Thus the applied microwave power is coupled effectively only in the discharge region, where a significant amount of seed charges exist. This approach was demonstrated in a previous work by Kuo *et al* [21]. Using an arc torch to produce seed plasma, a relatively large exit hole on the cavity surface can be used to increase the diameter of the torch. It reduces the Q -factor of the cavity; thus the evanescent microwave electric field can reach farther out of the cavity hole to also increase the height of the torch.

However, cavity-based microwave plasma torches are difficult to use as an igniter within a supersonic combustor. This difficulty results from the fact that the walls of the engine have a thickness of more than 50 mm and large openings on the walls are forbidden in order to minimize the perturbation on the supersonic flow in the combustor. In addition, as a practical matter, there are no large empty spaces adjacent to the walls for accommodating a microwave cavity.

In the present paper, a microwave-augmented plasma torch is developed. It combines an arc torch module with a rectangular microwave cavity in the form of a microwave adaptor. The torch module is used not only to generate the arc plasma but also to couple the microwave power from the cavity to the arc plasma for microwave enhancement. Most importantly, this torch module does not require the microwave cavity to be adjacent to the engine walls; it can still be easily plugged to the engine along with a required seal to high-pressure gas; and the required opening on the engine wall is the same as that for an arc torch. In section 2, the plasma torch module is described. A theoretical formulation and numerical analysis of the microwave coupling efficiency of this adaptor are presented in section 3. The experimental

results demonstrating the microwave effect on the electric characteristics and physical size of this plasma torch are presented in section 4. Finally, in section 5 summary and conclusions are given.

2. Description of the device

The components of this plasma torch device include (1) a 2.45 GHz, 1.5 kW magnetron as the microwave source, (2) a torch module, (3) a tapered microwave cavity and (4) a power supply to run the torch module and the magnetron

2.1. Arc torch module

The cylindrical torch module, which uses the frame of a cylindrical tube having an outer diameter of 16.5 mm as the grounded outer electrode, is first described. This torch module is similar to that developed by Kuo *et al* [15–17], with the exceptions that the device is longer and has an integrated gas plenum chamber allowing for the module to be integrated into a supersonic combustor. Moreover, the central electrode has been replaced with a tungsten carbide tube providing an additional flow path for either air or fuel. The concentric electrodes in the module are separated at the nozzle exit location by a gap of 2.16 mm and insulated by a ceramic tube, having outer and inner diameters of 9.53 mm and 3.81 mm, respectively, and dielectric constant $\epsilon_r = 8$, which hosts the central electrode. The frame, having a length of 14 mm, consists of three sections. The bottom section is 51 mm in length, having an inner diameter slightly larger than 9.53 mm to be fitted with the ceramic insulator. It is convenient to centre the central electrode hosted by the ceramic insulator. In the torch operation gas flow through the gap between electrodes is necessary. Thus, the central section having a length of 93 mm is open up to a much larger inner diameter of 12.7 mm so that this section functions as a gas plenum chamber. A threaded nozzle of 2 mm length is inserted at the top of the frame to increase the gas flow speed in the discharge region. This nozzle has an inner diameter of 7.5 mm. The ceramic insulator does not cover the central electrode in the nozzle. It is placed slightly below the bottom of the nozzle. The central electrode is a tungsten carbide tube with inner and outer diameters of 1.14 mm and 3.18 mm, respectively, and fits tightly inside the ceramic insulator. The hollow centre section can be connected to a separate gas supply allowing for an additional, independent flow path through the discharge region. The flow path through the centre of the tungsten carbide tube is used for injection of ethylene fuel in the present study. However, any gas can be used in either the inner or the outer flow paths. Figure 1(a) is a photo of a disassembled arc torch module showing its components; in the photo the labels are $A = 16.5$ mm, $B = 2$ mm, $C = 93$ mm and $D = 51$ mm as described earlier, where D includes the height of the module holder welded on top of the cavity. A photo of the assembled torch module is shown in figure 1(b).

2.2. Tapered rectangular waveguide cavity

An S-band rectangular waveguide having a cross section of $a \times b_0$ ($=72$ mm \times 34 mm) is tapered to a cross section of a

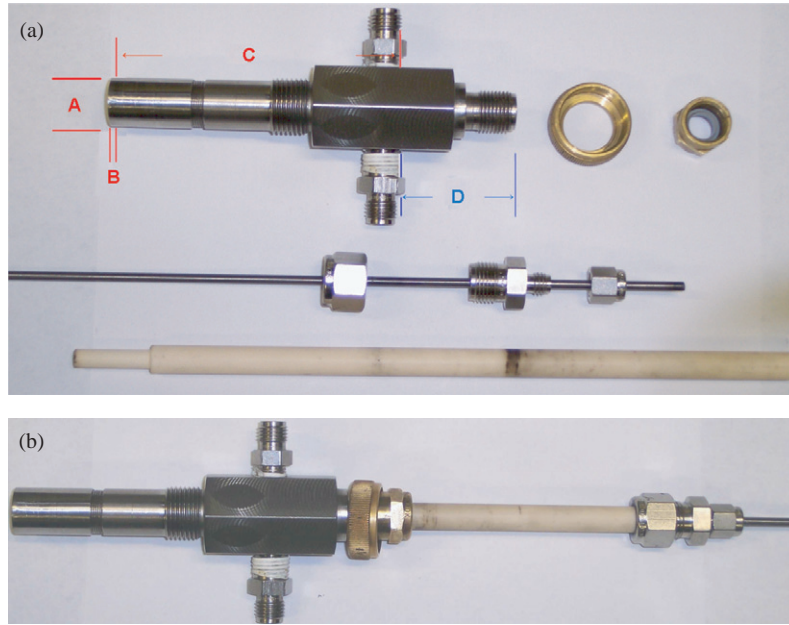


Figure 1. (a) A photo of the disassembled arc torch module showing its components; $A = 16.5$ mm, $B = 2$ mm, $C = 93$ mm and $D = 51$ mm. (b) A photo of the arc torch module.

$\times b$ ($=72$ mm \times 5 mm). The two ends of the waveguide are terminated by conducting plates to form a rectangular cavity. This cavity consists of three sections. Two sections with uniform cross section are connected by a tapered section. The first section (cross section of 72 mm \times 34 mm) has a length of $3\lambda_z/8$ and the last section (cross section of 72 mm \times 5 mm) has a length of $\lambda_z/2$ where $\lambda_z = \lambda_0/[1 - (\lambda_0/2a)^2]^{1/2} = 233$ mm is the axial wavelength for the TE₁₀₃ mode, $\lambda_0 = 122.5$ mm is the free space wavelength and $a = 72$ mm is the dimension of the wider side of the cross section. The middle transition section, tapering the cross section from 72 mm \times 34 mm to 72 mm \times 5 mm, has a length of $\lambda_z/2$ and a slope angle $\theta = 14^\circ$. This cavity is similar to the one used in a microwave torch device reported previously [21].

The microwave generated by a magnetron (2.45 GHz, 700 W to 1.5 kW) radiates into this cavity at a location about a quarter wavelength ($\lambda_0/4$) (more precisely, $\lambda_z/8$) away from the end-wall of the non-tapered section of the cavity. The quarter wavelength in the axial direction of the uniform sections of the cavity is 58.3 mm and the wavelength in the middle transition section is expected to be a little shorter; thus, the total axial length of 320 mm matches the length requirement for the TE₁₀₃ cavity mode. This result was confirmed by a measurement of the spatial distribution of the microwave electric field normal to the bottom wall of the cavity (figure 2 in [21]).

In the narrow section of the cavity, two aligned holes on the bottom and top walls of the cavity at a distance $\lambda_z/8 = 29.2$ mm away from the end are introduced. The top hole has a diameter of 9.53 mm and a tube fitting is welded to it. The arc torch module shown in figure 1(b) is then installed through the holder, as shown in the photo of figure 2, by inserting the bottom part containing only the central electrode and the ceramic insulator of the torch module through these two aligned holes. The bottom hole on the cavity wall has the same diameter of 9.53 mm fitted exactly to the ceramic insulator. The portion of the central electrode of the torch

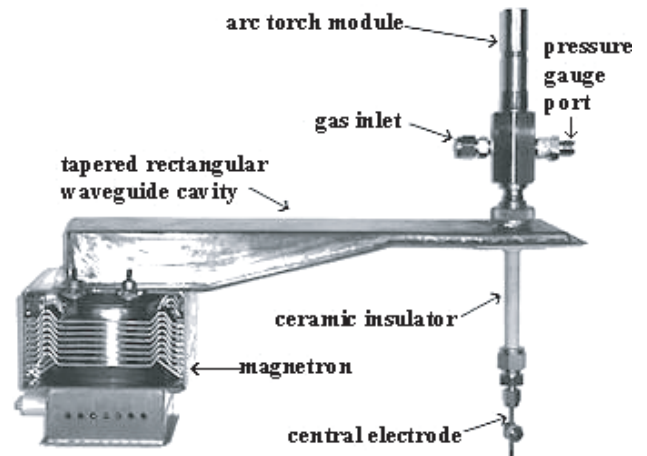


Figure 2. Photograph of the microwave-augmented plasma torch module.

module inside the cavity functions as a receiving antenna and the portion (~ 146 mm) of the torch module above the top wall of the cavity functions as an open-end transmission line. In this configuration, the plasma torch module becomes a microwave adaptor. In figure 2, a magnetron with its transmitting antenna inserted into the cavity from the other side (non-tapered section) is also shown. When plasma is generated by the arc discharge between the electrodes of the arc torch module, the plasma produces a time varying resistive load of the adaptor. The effectiveness of delivering the microwave through this adaptor to a dynamic load will be analysed and presented in the next section.

2.3. Power supply

The power supply consists of a high-power transformer, diodes and capacitors. The transformer uses a single-phase input from

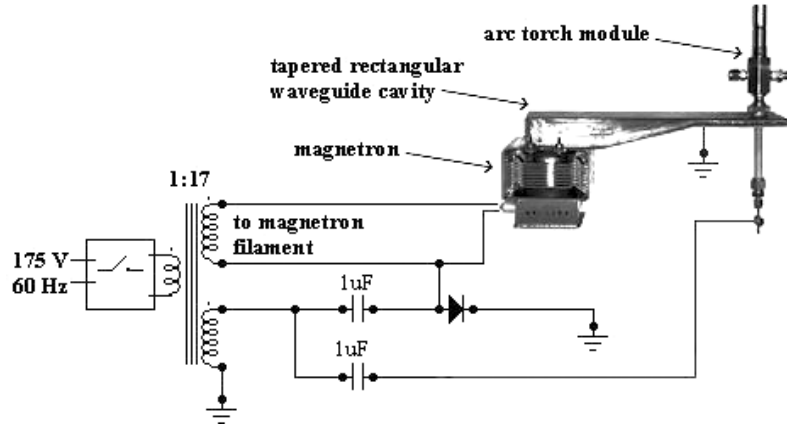


Figure 3. Schematic circuit diagram of the combined power supply.

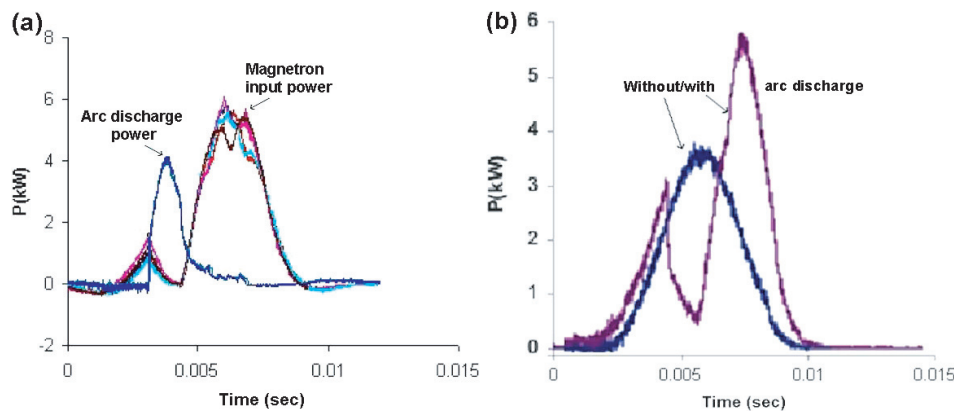


Figure 4. (a) Power functions of the arc discharge and magnetron input and (b) power functions of the magnetron input without and with arc discharge.

a 208 V power line and has a 1 : 17 turn ratio. This power supply initiates the arc discharge on the first cycle after power is applied to the transformer. However, a few seconds are required to heat up the filament of the magnetron before the torch operates in a microwave-augmented mode.

Both the torch module and magnetron operate at the power line frequency, typically 60 Hz, with less than 50% duty cycle. Hence, the synchronization of the two components in each cycle is essential to the operation of this hybrid torch module. The optimal operation condition is when the arc discharge pulse of the torch module and the microwave pulse of the magnetron overlap in time. The microwave field is too small to initiate discharge by itself for the microwave power used in the present setup. Since the discharge pulse is shorter than the microwave pulse, the arc discharge needs to start at the beginning of the steady-state level of the microwave pulse. Thus, the two components share the same power supply to simplify the synchronization.

Figure 3 shows a circuit diagram of the power supply used in this study, which is capable of operating the arc discharge and the magnetron simultaneously. A single power transformer with a turn ratio of 1 : 17 is used to step up the 60 Hz line voltage from 208 V (rms) to 3.5 kV (rms), which is applied to both the devices through two (one for each device) serially connected $1 \mu\text{F}/2.3 \text{ kVAC}$ capacitors. However, since neither device requires the full 3.5 kV (rms) in their operations, a

Variac (variable transformer) is used to reduce the input voltage from 208 to 175 V. The magnetron, which has a grounded anode, is then connected in parallel with a diode (15 kV and 750 mA rating) to assure that only negative voltages are applied to the cathode.

2.4. Performance of the power supply

The arc discharge occurs in both the positive and negative voltage cycles of the ac input; the plasma generated during negative-voltage discharges directly interacts with the magnetron output pulses and the plasma generated during the positive-voltage discharges interacts with the remaining microwave energy stored in the cavity.

The arc discharge draws too much current from the power supply for the capacitor in the magnetron circuit to maintain the required voltage for turning on the magnetron. Consequently, the magnetron is automatically turned off during the peak of arc discharge. This effect is demonstrated in figures 4(a) and (b), which presents the synchronized power functions of the negative arc discharge and magnetron input as well as the power functions of the magnetron input power with and without the arc discharge. As shown, the magnetron operation is interrupted by the arc discharge. However, the arc discharge still provides seed charges to interact with the main pulse of the microwave, which extends the duration of the plasma

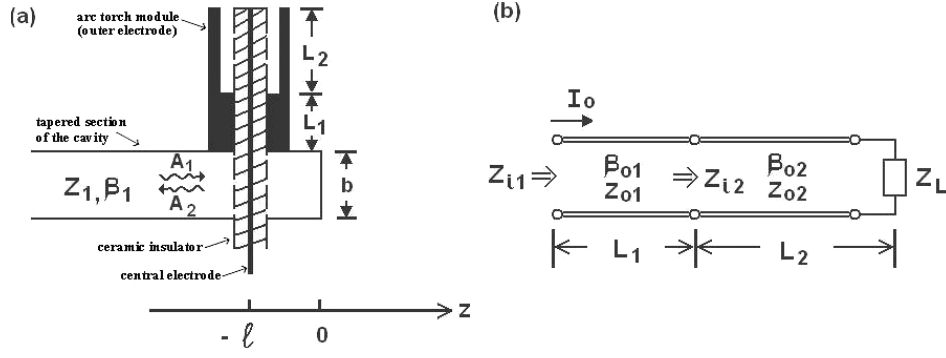


Figure 5. (a) Schematic of the microwave adaptor and (b) equivalent transmission line model of the arc torch module.

pulse. Unfortunately, the total duration of the microwave-augmented plasma cannot be monitored by the arc current measurement. After the discharge, the voltage returns to a high value, and the output power of the ‘restarted’ magnetron increases considerably as seen in figure 4(b). The coupling of the two loads improves the power factor of the power line from 0.52 to 0.89. It is noted that the results presented in figure 4 were obtained from low power operation of the device, where the input was from the 120 V power line, rather than from the 208 V line used to obtain the higher power results presented in section 4.

3. Coupling efficiency

3.1. Model of the arc torch module

The torch module has a coaxial structure and can easily be connected to a rectangular waveguide of a cross section ($a \times b$) to form a microwave adaptor. A schematic of such an arrangement is shown in figure 5(a). In this adaptor, the antenna size is equal to b , the dimension of the short side of the waveguide, because the central electrode of the module has to pass through the waveguide to be accessible to high voltage connection for the arc discharge. This size is different from that of the conventional adaptor, which is usually less than $b/2$. Two serially connected transmission lines shown in figure 5(b) are used to represent the torch module; that is, the detail of the short nozzle section of the torch module, which is much shorter than the wavelength, is not included in the analysis. The central electrode is tightly fit to the ceramic insulator so that no air gap exists between the two components. The characteristic impedances Z_0 and propagation constants β_0 of these two transmission lines are determined to be [22]

$$Z_{01} = (60/\sqrt{\epsilon_r}) \ln(r_{01}/r_i)\Omega,$$

$$Z_{02} = 60\{\ln(r_{02}/r_i)[\epsilon_r^{-1} \ln(r_{01}/r_i) + \ln(r_{02}/r_{01})]\}^{1/2}\Omega, \quad (1)$$

$$\beta_{01} = k_0\sqrt{\epsilon_r},$$

$$\beta_{02} = k_0\{\ln(r_{02}/r_i)/[\epsilon_r^{-1} \ln(r_{01}/r_i) + \ln(r_{02}/r_{01})]\}^{1/2},$$

where $k_0 = \omega_0/c$ is the wave number in free space, ω_0 is the wave angular frequency, c is the speed of light in free space, r_i and r_{01} are the outer radii of the central electrode and the ceramic insulator, respectively, and r_{02} is the inner radius of the gas plenum chamber (central section of the torch frame).

When the arc discharge is initiated, a time varying plasma is generated to be the load of the transmission line. The generated plasma acts as a resistive load to absorb the microwave power as well as an antenna to radiate the microwave power. Therefore, it is practical to consider plasma as a time varying resistive load of the combined line, represented by R_L which is the sum of the plasma resistance and the radiation impedance (resistance) of the plasma antenna. For safety reasons, a microwave leakage detector (MD-2000) was used in experiments to monitor the level of the microwave flux. It was found that the power flux at 1 m distance away was less than 1 mW cm^{-2} , which was within the safety threshold level of 5 mW cm^{-2} . The radiated power was estimated to be less than 5% of the magnetron input power. The antenna inside the waveguide receives the microwave power to make a current source as the input of the line. The microwave power coupling efficiency depends on the matching condition of the load. However, plasma is a dynamic load, i.e. a time varying resistive load, so perfect impedance matching over the operational range is not possible. In the following, an analysis to determine the dependence of the coupling efficiency on R_L is presented.

3.2. Analysis

The input impedances of line 1 and line 2 are Z_{i1} and Z_{i2} as shown in figure 5(b). Introducing the normalized impedances $z_{i1} = Z_{i1}/Z_{01}$, $z_{i2} = Z_{i2}/Z_{02}$ and $z_l = Z_L/Z_{02}$, and the notations $a_1 = \tan \beta_{01}L_1$, $a_2 = \tan \beta_{02}L_2$ and $\eta = Z_{02}/Z_{01}$, allows the input impedances to be expressed as

$$z_{i1} = (\eta z_{i2} + j a_1)/(1 + j \eta z_{i2} a_1) \quad (2)$$

and

$$z_{i2} = (z_l + j a_2)/(1 + j z_l a_2). \quad (3)$$

Substituting equation (3) into equation (2), the following expression is obtained for the input impedance

$$z_{i1} = [z_l(\eta - a_1 a_2) + j(\eta a_2 + a_1)]/[(1 - \eta a_1 a_2) + j z_l(\eta a_1 + a_2)] = R_{i1} + j \chi_{i1}. \quad (4)$$

The input impedance z_{i1} of the combined line given by equation (5) represents the load impedance of the antenna which is expressed as a function of the actual load impedance z_l of the system. Considering only TE_{10} mode in the waveguide of figure 5(a), the phasors of the wave fields are

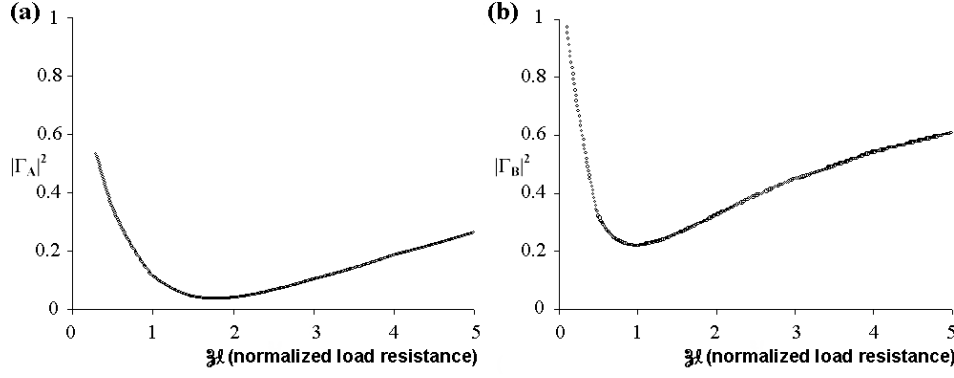


Figure 6. Reflectance $|\Gamma|^2$ of the adaptor as a function of the normalized load resistance $z_l (= Z_L/Z_{02})$ for two different torch module locations: (a) $l = \lambda_z/8$ and (b) $\lambda_z/4$ from the endplate, where $Z_{02} = 47.4 \Omega$.

given by

$$\sin(\pi x/a)[A_1 \exp(-j\beta_1 z) + A_2 \exp(j\beta_1 z)] \quad \text{for } z < -l,$$

$$\begin{aligned} \mathbf{E} &= \hat{\mathbf{y}} \sin(\pi x/a)[A_1 \exp(-j\beta_1 z) + A_2 \exp(j\beta_1 z)] \\ &\quad \text{for } z < -\ell \\ &= \hat{\mathbf{y}} B \sin(\pi x/a) \sin(\beta_1 z) \quad \text{for } -\ell < z < 0 \end{aligned} \quad (5)$$

$$\begin{aligned} \mathbf{H} &= \hat{\mathbf{x}} Z_1^{-1} \sin(\pi x/a)[A_1 \exp(-j\beta_1 z) - A_2 \exp(j\beta_1 z)] \\ &\quad \text{for } z < -\ell \\ &= -j\hat{\mathbf{x}} Z_1^{-1} B \sin(\pi x/a) \cos(\beta_1 z) \\ &\quad \text{for } -\ell < z < 0 \end{aligned} \quad (6)$$

where $Z_1 = \omega_0 \mu_0 / \beta_1 = \eta_0 k_0 / \beta_1$ is the wave impedance in the waveguide; μ_0 is the free space permeability, $\eta_0 = 377 \Omega$ is the intrinsic impedance of the free space and $\beta_1 = 2\pi/\lambda_z$ is the wave propagation constant in the waveguide; $A_2 = \Gamma A_1$, where $\Gamma = \Gamma_r + j\Gamma_i$ is the reflection coefficient. $\Gamma = 0$ only when the load is matched to the line and the reflectance $|\Gamma|^2$ determines the coupling efficiency (given by $1 - |\Gamma|^2$). The continuity condition of the wave electric field at $z = -l$ leads to $A_1 \exp(j\beta_1 l) + A_2 \exp(-j\beta_1 l) = -B \sin(\beta_1 l)$, which reduces to $B = -(\sin \beta_1 l)^{-1} [1 + \Gamma \exp(-2j\beta_1 l)] A_1 \exp(j\beta_1 l)$.

This wave electric field induces an antenna current density given by

$$\mathbf{J} = \hat{\mathbf{y}} I_0 \sin(\pi y/2b) \delta(x - a/2) \delta(z + l) \quad \text{for } 0 \leq y \leq b, \quad (7)$$

where $y = 0$ and $y = b$ are located on the bottom and top plates of the waveguide shown in figure 5(a), respectively. At $y = b$, the antenna current is $I = I_0$, which is the input current of the combined transmission line shown in figure 5(b). The net time-average microwave power received by the antenna is given by

$$P_0 = -\frac{1}{2} \int \mathbf{E} \times \mathbf{H}^* \cdot d\mathbf{S} = \frac{1}{2} \int \mathbf{E} \cdot \mathbf{J}^* dV. \quad (8)$$

This power should equal to the net input power of the transmission line, which is given by $\frac{1}{2} |I_0|^2 Z_{i1}$. Thus the power balance condition leads to the following equation:

$$-\frac{1}{2} \int \mathbf{E} \times \mathbf{H}^* \cdot d\mathbf{S} = \frac{1}{2} \int \mathbf{E} \cdot \mathbf{J}^* dV = \frac{1}{2} |I_0|^2 Z_{i1}. \quad (9)$$

Substituting equations (5)–(7) into equation (9), results in two coupled real equations for Γ_r and Γ_i being obtained.

The coefficients of the equations are functions of the variable parameter l and the location of the antenna (torch module). These coefficients are simplified by considering two preferential locations: $l = \lambda_z/8$ and $\lambda_z/4$, i.e. $\beta_1 l = \pi/4$ and $\pi/2$.

Case A. $l = \lambda_z/8$. The coupled equations are given by

$$(1 - \Gamma_r^2 - \Gamma_i^2)/(1 + \Gamma_r^2 + \Gamma_i^2 + 2\Gamma_r + 2\Gamma_i) = -R_{i1}/\chi_{i1} \quad (10)$$

and

$$\begin{aligned} (1 + \Gamma_r + \Gamma_i)[(1 + \Gamma_i)^2 + \Gamma_r^2]/[(1 - \Gamma_r^2 - \Gamma_i^2)^2 \\ + (1 + \Gamma_r^2 + \Gamma_i^2 + 2\Gamma_r + 2\Gamma_i)^2] \\ = (\pi^2 a Z_{01}/16b Z_1)(R_{i1} - \chi_{i1}), \end{aligned} \quad (11)$$

where R_{i1} and χ_{i1} , given by equation (5), are functions of the load impedance z_l .

Case B. $l = \lambda_z/4$. The coupled equations become

$$(1 - \Gamma_r^2 - \Gamma_i^2)/2\Gamma_i = -R_{i1}/\chi_{i1}, \quad (12)$$

$$\begin{aligned} [(1 - \Gamma_r)^2 + \Gamma_i^2]^2/[(1 - \Gamma_r^2 - \Gamma_i^2)^2 + 4\Gamma_i^2] \\ = (\pi^2 a Z_{01}/8b Z_1)^2 |z_{i1}|^2. \end{aligned} \quad (13)$$

These two sets of two equations [(10) and (11), and (12) and (13)] will be solved to obtain $|\Gamma|^2(z_l)$ for comparison.

3.3. Numerical results

Using the dimensions of the torch device presented in this work yields $Z_{01} = 24.5 \Omega$, $Z_{02} = 47.4 \Omega$, $Z_1 = 682 \Omega$, $\beta_{01} = 2.83 k_0$, $\beta_{02} = 1.83 k_0$ and $\beta_1 = 1.81 k_0$, where $k_0 = 16.33\pi \text{ m}^{-1}$, $a = 72 \text{ mm}$ and $b = 5 \text{ mm}$. Thus $a_1 = 2.1$, $a_2 = -0.72$ and $\eta = 1.93$, which reduces equation (5) to $z_{i1} = [1.03z_l + j(0.18 - 0.75z_l^2)]/(1 + 0.72z_l^2) = R_{i1} + j\chi_{i1}$. With the aide of these parametric values, equation sets (10) and (11) and (12) and (13) are solved numerically. The results $|\Gamma_A|^2(z_l)$ and $|\Gamma_B|^2(z_l)$ are presented in figures 6(a) and (b), respectively. As shown in the figures, $|\Gamma_A|^2 < |\Gamma_B|^2$; moreover, $|\Gamma_A|^2 < 0.2$ for $38 \Omega < Z_L < 200 \Omega$, while $|\Gamma_B|^2 > 0.2$ in the same region. This impedance region corresponds to the times before and after the peak of the arc discharge. In the setup, the magnetron and the arc torch module share the same power supply to eliminate the need of an additional circuit to synchronize the microwave pulse with the arc discharge. Hence, the magnetron operation is affected by the arc discharge, which causes voltage to drop considerably.

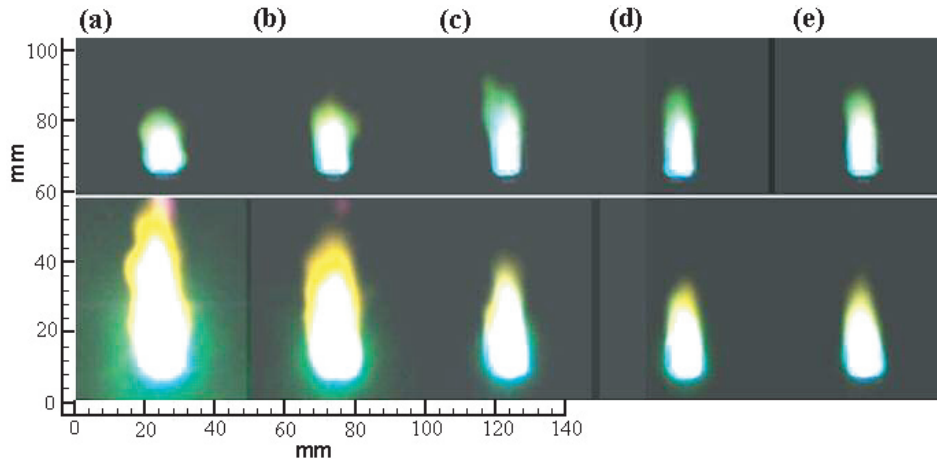


Figure 7. Images of plasma plumes generated before (top row) and after (bottom row) the magnetron is turned on. The air supply pressures in (a) to (e) are 1.36, 2.04, 3.4, 4.76 and 5.44 atm.

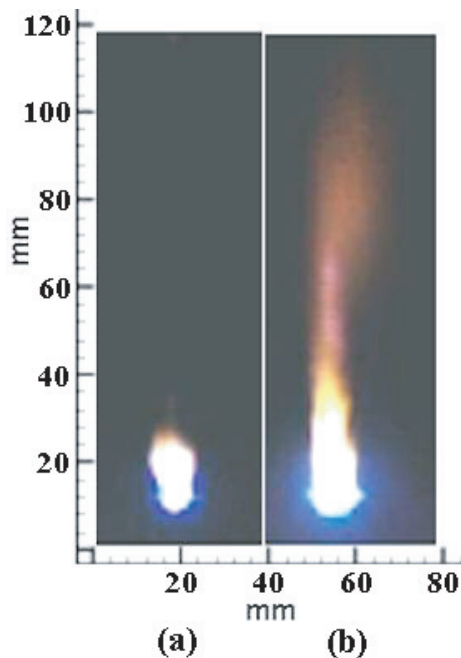


Figure 10. Torch plasma plumes: (a) air plasma generated by arc discharges and (b) flame plume (in the centre) ignited by a 60-Hz microwave plasma torch; in both the cases gaseous ethylene fuel (flow rate of 20 SLM) was injected through the central electrode (tungsten-carbide tube) and an airflow rate of 30 SLM was supplied.

As shown in the preceding section, the magnetron is off during the peak of the arc discharge due to the voltage drop during the arc discharge. In other words, during the high reflectance time period when the plasma torch has very low impedance, the voltage drop automatically shuts off the magnetron. This automatic shutoff feature also improves the coupling efficiency of this microwave adaptor. The results presented in the next section are obtained using Case A arrangement with $l = \lambda_z/8$.

4. Microwave effects on the plasma torch

The torch is operated in open air using compressed air as the feedstock. The torch module operates stably over a very large

flow rate range, with flow speeds from subsonic to supersonic. The effects of microwave power on the plasma torch, which vary with the gas flow rate, include the following.

4.1. The size and enthalpy of the plasma torch

This effect together with its dependence on the gas flow rate is demonstrated by the single frame CCD plasma plume images shown in figure 7. The five sets of images with the microwave off (top row) and on (bottom row) from (a) to (e) correspond to the air supply pressures of 1.36 atm, 2.04 atm, 3.4 atm, 4.76 atm and 5.44 atm absolute, respectively, where the flow speeds at the nozzle exit of the torch module are subsonic in (a) to (c) and are supersonic in (d) and (e). As shown in the figure, the applied microwave power can increase the height and the volume of the plasma torch significantly at low gas flow rates. Comparing the top- and bottom-row plume images in (a) to (e), it is seen that, with the application of microwave power, the respective plume heights increase by more than 300%, 100%, 30%, 20% and 10% and the respective plume volumes increase by approximately 900%, 400%, 180%, 100% and 50%. The enhancement is estimated from the increased luminosity of the plasma plume, which provides an indirect measurement. The effect of applying the microwave power decreases with increasing flow speed. As the air supply pressure is increased, thereby increasing the flow speed, the size of the arc plasma torch shown in the top row of figure 7 also increases except at the transition from subsonic (c) to supersonic (d). Alternatively, the plume sizes of the microwave-enhanced plasma torches shown in the bottom row of figure 7 decrease with increasing flow speed but are still enhanced compared with the arc only images as indicated by lower luminosity of the arc only plasma plumes. This dependence most likely results from the fact that the fixed applied power has to energize more gas with less interaction time as the flow rate increases and that the size of the plasma torch becomes dictated by the flow speed. At the same supply of pressure, the heights of the microwave-augmented plasma torches shown in (d) and (e) are only slightly larger than the corresponding arc plasma torches. However, the volume and the luminosity intensity of the plasma plume are still increased by the application of the microwave power.

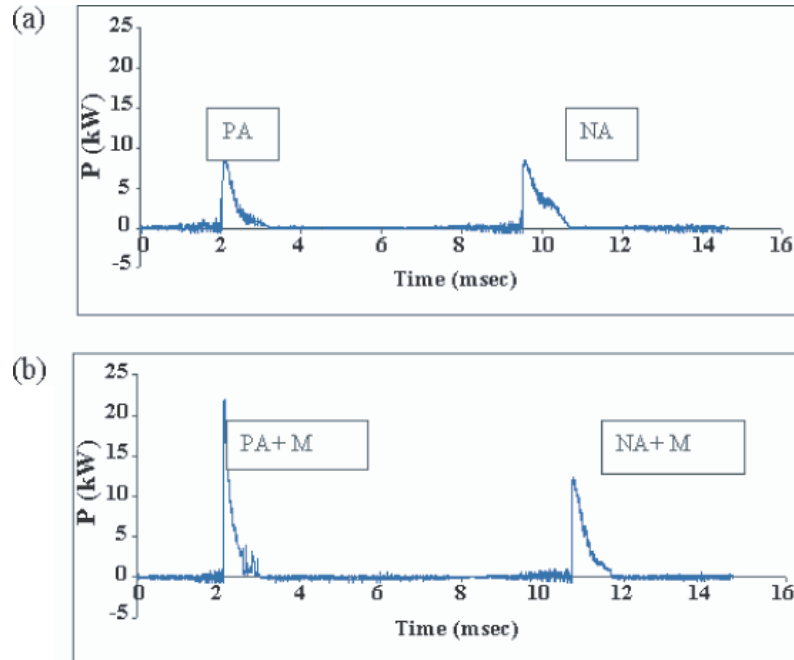


Figure 8. The power of the 60 Hz arc discharge. (a) The positive arc (PA) and negative arc (NA). (b) The microwave field applied to the positive arc (PA + M) and the negative arc (NA + M).

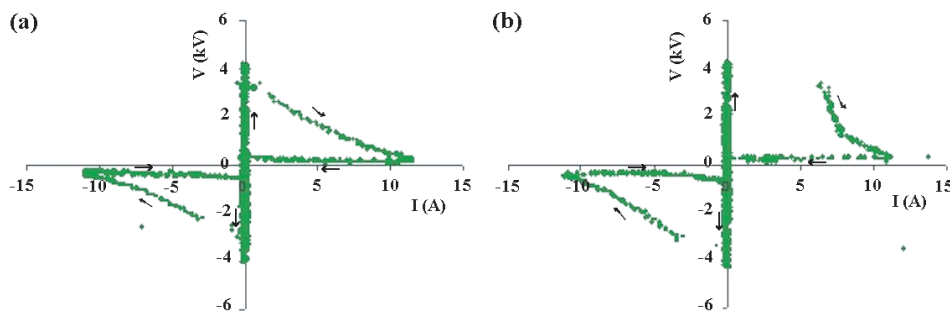


Figure 9. $V-I$ characteristics of discharges (a) without the microwave and (b) with the microwave.

4.2. The electric characteristics of the plasma torch

The time varying voltage V and current I of the discharge were measured using a digital oscilloscope (Tektronix TDS3012 DPO 100 MHz and 1.25 GS^{-1}). The product of the V and I functions gives the instantaneous power function. The arc discharge occurs in each half-cycle, but the magnetron runs only during the negative-voltage half-cycle. Thus, the microwave pulse lasting approximately 6 ms is expected to synchronize only with the negative discharge pulse. However, the operation of the magnetron is affected by the arc discharge. In fact, as shown in figure 3(a), the magnetron is shut off during the main pulse of the arc discharge. It turns out that the microwave effect on the positive discharge is stronger than that on the negative discharge in the case of a low flow rate. The power functions in one cycle for discharges without and with the presence of the microwave in the case of a low flow rate are presented in figures 8(a) and (b) for comparison. The supply pressure of the torch module is 1.16 atm. The powers plotted in figure 8 are calculated from the current drawn by the arc discharge and the voltage drop across the two electrodes, i.e. no contribution from the magnetron is included.

As shown, the microwave has enhanced both the peak power of the negative discharge and the positive discharge. The peak power in the negative discharge pulse is increased from 8 to 12 kW. However, the total energy per pulse does not increase proportionally, because the discharge pulse energy is limited by the available energy stored in the capacitors, which does not change significantly. In the arc discharge, the voltage and current peaks are not in phase. The voltage reaches the peak of about 4 kV when the gaseous breakdown starts. As the discharge current increases, the discharge voltage drops rapidly to a relatively low level in the range 200–400 V. Thus, at the peak current the discharge voltage is, in fact, quite low, which limits the peak discharge power. The microwave helps to reduce the phase delay of the current peak from the voltage peak resulting in a higher discharge voltage while the discharge current is increasing. The $V-I$ characteristic plots shown in figures 9(a) and (b), for discharges without and with the presence of microwave, respectively, also demonstrate this point. As indicated the peaks of the arc discharge currents in both cases are about the same. However, the areas of the hysteresis loops in figure 9(b) are larger than the corresponding ones in figure 9(a) and the arc discharge voltages at large

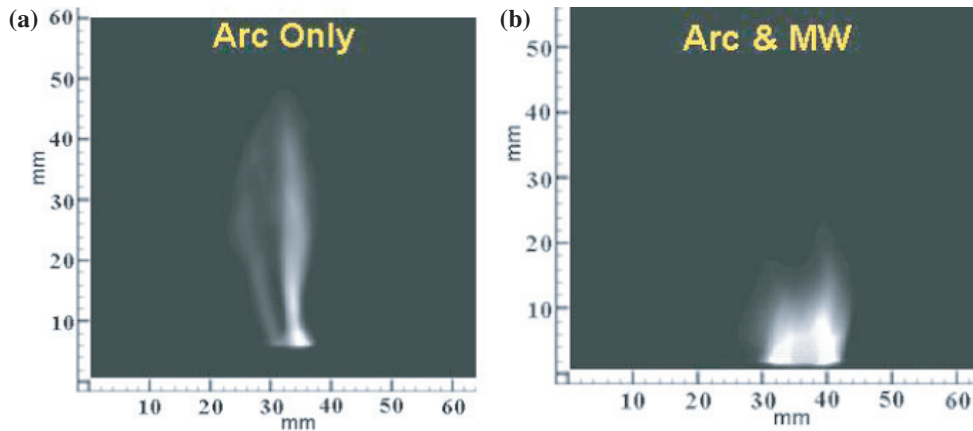


Figure 11. Plasma plume emission images recorded with an interline-transfer CCD camera image with an $100\ \mu\text{s}$ exposure; the illuminated portions shown correspond to the discharge region generated by (a) an arc discharge and (b) an arc discharge in the presence of the microwave.

current values (figure 9(b)) are higher. Consequently, the peak of the product of V and I functions is increased. It is also indicated in figure 9(b) that microwave considerably increases the breakdown voltage in the positive discharge. It is understood that the discharge initiates in the region near the central electrode where the applied electric field concentrates due to the cylindrical geometry. When the central electrode is positive, it collects electrons produced close to it by the discharge. The microwave field introduces radially quiver motions in electrons. Since the microwave frequency is much smaller than the electron collision frequency, the mean free path of electrons is essentially determined and thus enhanced by the quiver speed; this then increases the transit-time loss of electrons to the central electrode, which in turn increases the breakdown voltage. The microwave effect on the positive discharge is likely attributed to the circuit arrangement and cavity setup. The negative arc discharge delays the start of the magnetron as shown in figure 4(a) and the cavity prolongs the storing time of the remaining microwave after the negative arc discharge.

4.3. The ignition capability of the plasma torch

Experiments demonstrating the torch module as a fuel injector and igniter of hydrocarbon fuel have also been performed. Tests have been conducted using gaseous ethylene fuel with the flow rate of 9 standard litres per minute (SLM) injected through the central electrode, a tungsten-carbide tube, corresponding to $160\ \text{m s}^{-1}$ fuel velocity at 298 K. The flame plume was observed when the torch was run with airflow rates ranging from 10–100 SLM with microwave power applied. This airflow rate range corresponded to air velocities of 6–65 m s^{-1} at 298 K. Ignition under these conditions is illustrated in figure 10(b). The plasma plume of the arc discharge (without microwave) operated in the same condition is shown in figure 10(a) for comparison. As shown, the fuel was not ignited in figure 10(a). This effect is understood because fuel was injected from the central port of the module, which is outside the main arc discharge region. An estimate of the discharge region can be seen in the images shown in figure 11. Figure 11(a) is the arc plasma plume emission image recorded with an interline-transfer CCD camera with a $100\ \mu\text{s}$ exposure.

This image was recorded through a 1 nm bandpass interference filter centred at 405 nm, and the high intensity region was correlated to energy deposition by the plasma. The use of a narrow bandpass filter was necessary in order to prevent saturation of the CCD camera allowing the discharge region to be clearly imaged. As the microwave is introduced, the plasma torch distributes more uniformly across the electrodes as seen in figure 11(b), i.e. the discharge becomes more cylindrical. In figure 11(b), the plasma distribution is more uniform and has a higher density in the central region of the hollow central electrode where the fuel is ejected. The microwave energy has also significantly enhanced the size and enthalpy (evidenced by the luminosity contrast shown in figure 7) of the plasma torch. It is noted that the arc discharge alone can ignite the fuel by increasing the discharge energy through increasing the capacitance in the power circuit of the arc discharge from 1 to 3 μF and through increasing the airflow rate. Maintaining the ethylene flow rate at 9 SLM, fuel was ignited with a maximum of 400 SLM airflow rate.

The results presented in figures 10(b) and 11(b) demonstrate that the microwave-augmented arc discharge operating with low airflow rate can deliver enough energy to the gas over a larger volume to ignite the fuel. Low airflow rate operation is an essential requirement of a practical igniter.

5. Summary and conclusions

A torch device that integrates a cylindrical-shaped plasma torch module into a tapered rectangular microwave cavity is described. The central electrode of the torch module is inserted through the tapered side of the cavity at $\lambda_z/8$ distance away from the end wall to function as a receiving antenna, and the microwave power injected into the cavity from the other end is delivered to the plasma torch generated by the torch module through this coupling. In the presence of seed charges provided by the arc discharge, the required microwave field intensity for the initiating the microwave discharge is well below the microwave breakdown threshold field. Thus, the present microwave-augmented torch module employs a power level low enough to avoid undesired microwave breakdown inside the cavity but high enough to introduce significant microwave enhancement of the arc discharge.

A theoretical analysis of the microwave coupling efficiency shows that nearly 80% of the supplied microwave power can be delivered to the arc plasma through this adaptor arrangement. Experiments performed demonstrate that the added microwave energy increases the height and volume of the plasma torch considerably. The magnitude of the microwave enhancement decreases as the airflow rate increases. Nevertheless, the height and the volume of microwave-augmented plasma torch exceed those of the arc plasma torch even when the flow speed is supersonic. The added microwave power also affects the peak power delivered by the arc discharge by affecting the phase relationship of the current and voltage. The addition of the magnetron to the circuit increases the circuit efficiency enabling more power to be delivered to the gas.

The three principal advantages of the microwave-augmented device discussed here are that (1) it is compact and durable, running for long periods of time in a periodic mode on an air feedstock; (2) it needs very low gas flow rate in its operation, which is an essential requirement of a practical igniter and (3) it is able to run as a combined igniter/fuel injector. The microwave-augmented arc discharge operating with a low gas flow rate delivers more energy to the gas over a larger volume, as evidenced by the measured powers and luminosity of the plasma plume, compared with previous arc discharge configurations. This improvement should prove beneficial for applications involving both ignition and combustion in a variety of environments.

Acknowledgments

This work was supported by Air Force Office of Scientific Research (AFOSR) Grant AFOSR-FA9550-04-1-0352 and a laboratory task LRIR-02PR02COR.

References

- [1] Boulou M I, Fauhais P and Pfender E 1994 *Thermal Plasma Fundamentals and Applications* vol 1 (New York: Plenum) pp 33–47 and pp 403–18
- [2] Mitsuda Y, Yoshida T and Akashi K 1989 *Rev. Sci. Instrum.* **60** 249
- [3] Solonenko O P (ed) 2001 *Thermal Plasma Torches and Technologies* vol 1 (Cambridge: Cambridge International Science Publishers)
- [4] Herrmann H W, Henins I, Park J and Selwyn G S 1999 *Phys. Plasmas* **6** 2284
- [5] Laroussi M 2002 *IEEE Trans. Plasma Sci.* **30** 1409
- [6] Lai W, Lai H, Kuo S P, Tarasenko O and Levon K 2005 *Phys. Plasmas* **12** 023501(1-6)
- [7] Wagner T, O'Brien W, Northam G and Eggers J 1989 *J. Propul. Power* **5** 548
- [8] Masuya G, Kudou K, Komuro T, Tani K, Kanda T, Wakamatsu Y, Chinzei N, Sayama M, Ohwaki K and Kimura I 1993 *J. Propul. Power* **9** 176
- [9] Jacobsen L S, Carter C D and Jackson T A 2003 *AIAA Paper* 2003-0871 (American Institute of Aeronautics and Astronautics, Washington DC)
- [10] Mathur T, Streby G, Gruber M, Jackson K, Donbar J, Donaldson W, Jackson T, Smith C and Billig F 1999 *AIAA Paper* 99-2102 (American Institute of Aeronautics and Astronautics, Washington DC)
- [11] Gruber M, Jackson K, Mathur T and Billig F 1999 *XIV Int. Symp. on Air Breathing Engines (ISABE) (Florence, Italy)* Paper IS-7154
- [12] Gage R M 1961 Arc torch and process *United States Patent No* US2858411
- [13] Koretzky E and Kuo S P 1998 *Phys. Plasmas* **5** 3774
- [14] Reed T B 1961 *J. Appl. Phys.* **22** 821
- [15] Kuo S P, Koretzky E and Orlick L 2001 Methods and apparatus for generating a plasma torch *United States Patent No* US 6329628 B1
- [16] Kuo S P, Koretzky E and Orlick L 1999 *IEEE Trans. Plasma Sci.* **27** 752
- [17] Kuo S P, Bivolaru D, Carter C D, Jacobsen L and Williams S 2004 *IEEE Trans. Plasma Sci.* **32** 262
- [18] Yee J H, Alvarez R A, Mayhall D J, Byrne D P and DeGroot J 1986 *Phys. Fluids* **29** 1238
- [19] Goode S R and Otto D C 1980 *Spectrochim. Acta. B* **35** 569
- [20] Woskov P P and Hadidi K 2002 *IEEE Trans. Plasma Sci.* **30** 156
- [21] Kuo S P, Bivolaru D, Lai H, Lai W, Popovic S and Kessaratikoon P 2004 *IEEE Trans. Plasma Sci.* **32** 1734
- [22] Pozar D M 2005 *Microwave Engineering* 3rd edn (New York: Wiley)
- [23] Marcuvitz N 1951 *Waveguide Handbook* (New York: McGraw-Hill)